ARTICLE IN PRESS

Available online at www.sciencedirect.com

ScienceDirect

Proceedings of the Combustion Institute xxx (2014) xxx–xxx

Proceedings of the Combustion Institute

www.elsevier.com/locate/proci

"Third-Body" collision efficiencies for combustion modeling: Hydrocarbons in atomic and diatomic baths

Ahren W. Jasper [a,*], C. Melania Oana [a], James A. Miller [b]

[a] Combustion Research Facility, Sandia National Laboratories, Livermore, CA 94551, USA
[b] Chemistry Division, Argonne National Laboratory, Argonne, IL 60439, USA

Abstract

The collisional energy transfer dynamics relevant to the unimolecular kinetics of linear, branched, and cyclic hydrocarbons, including both radicals and saturated and unsaturated molecules, in atomic and diatomic baths is studied via classical trajectories. A set of full-dimensional potential energy surfaces (PESs) suitable for efficient trajectory simulations involving large hydrocarbons (C_xH_y) colliding with any of seven baths (M = He, Ne, Ar, Kr, H_2, N_2, O_2) is validated against direct dynamics calculations for two small systems. The PESs are then used to calculate Lennard-Jones collision parameters, and a general rule for calculating these parameters based only on the number of carbon atoms and the bath gas is obtained. Next, the PESs are used to calculate low-order moments of the collisional energy transfer function relevant to low-pressure-limit unimolecular kinetics for a total of 266 systems (38 unimolecular reactants in 7 baths), with a focus on the average angular momentum and total energy transferred in deactivating collisions. These moments are used to quantify the relative rotational and total collision efficiencies of the 7 baths for the various hydrocarbon reactants. Trends in the collision efficiencies with respect to the chemical structures of the hydrocarbon reactants are discussed.
© 2014 The Combustion Institute. Published by Elsevier Inc. All rights reserved.

Keywords: Classical trajectory simulations; Unimolecular kinetics; Bath gas efficiencies; Weak collider; Angular momentum

1. Introduction

In the low-pressure limit of a unimolecular reaction, the reaction rate is proportional to the rate of activating bath gas collisions and is therefore proportional to the pressure of the bath gas [1]. The relative collision efficiency $\mathscr{M}_M$ with which different bath gases M promote a unimolecular reaction may be formally defined as the ratio of low-pressure limit rate coefficients, k_0, i.e. $\mathscr{M}_M \equiv k_{0,M}/k_{0,Ar}$, where we have chosen Ar as the reference bath.

Few systematic experimental studies of $\mathscr{M}_M$ for unimolecular reactions in several baths have appeared (for example [2–4]), and the dependence of $\mathscr{M}_M$ on the temperature, bath gas, and chemical structure of the unimolecular reactants has not been widely quantified, particularly for unimolecular reactants with more than a few heavy atoms. Theoretical studies have also appeared

* Corresponding author. Fax: +1 (925) 294 2276.
E-mail address: ajasper@sandia.gov (A.W. Jasper).

http://dx.doi.org/10.1016/j.proci.2014.05.105
1540-7489/© 2014 The Combustion Institute. Published by Elsevier Inc. All rights reserved.

Please cite this article in press as: A.W. Jasper et al., *Proc. Combust. Inst.* (2014), http://dx.doi.org/10.1016/j.proci.2014.05.105

(for example [5–8]), but the majority of these have not been targeted at quantitative kinetics. We have studied the pressure-dependent kinetics of $CH_4 + M$ in ten atomic, diatomic, and molecular baths via a first-principles approach that includes classical trajectories, transition state theory, quantum chemistry, and master equation (ME) calculations [9–11]. The theoretical rate coefficients were found to agree with available experimental results within a factor of two, with the principal sources of error assigned to the neglect of vibrational anharmonicity and simplifications in the ME model for energy transfer. The principal goal of the present work is to use these methods, along with a new set of computationally efficient $C_xH_y + M$ potential energy surfaces (PESs), to characterize $\mathscr{M}_M$ for hydrocarbons as large as C_8H_{18} and for seven typical atomic and diatomic baths.

$\mathscr{M}_M$ can be calculated by solving the ME [12–14] for k_0 or approximately by evaluating simple functions of trajectory-based low-order moments of the energy transferred in bath gas collisions. In Ref. [11], $\mathscr{M}_M$ was evaluated using a one-dimensional (1D) and two different two-dimensional (2D) ME models. One of the 2D models (labeled 2D/φ) makes use of a microcanonical statistical assumption for the distribution of post-collision rotational states to simplify the solution of the ME. The other model (labeled 2D) is explicitly 2D and includes the effect of "weak collisions in J" that do not fully equilibrate rotations. For $CH_4 + He$ at 300 K, the weak-collider-in-J effect was found to lower k_0 by a factor of 2 (i.e., $k_0(2D/\varphi)/k_0(2D) = 2$). At higher temperatures, the results of the 2D/φ model agreed well with the 2D model, even when the trajectory results showed that rotations were not fully collisionally equilibrated microcanonically. Here, we quantify the efficiency of rotational equilibration for several baths and for hydrocarbons larger than methane.

Also shown in Ref. [11], solutions to the 1D ME were found to predict accurate *relative* collision efficiencies, $\mathscr{M}_M$, particularly for atomic and diatomic baths, even when the 1D and 2D values of k_0 differed significantly. Troe's weak collider correction, β_c, to the strong collider rate coefficient was derived [1] by considering solutions to the 1D ME, where $\beta_c = [\alpha/(\alpha + F_E k_B T)]^2$, F_E is related to the thermal population of the states of the unimolecular reactant above its reaction threshold, and α is the range parameter of the exponential energy transfer function P for deactivating collisions. For this choice of P and under conditions often satisfied for unimolecular kinetics, α is equal to the average energy transferred in deactivating collisions $\langle\Delta E_d\rangle$. Within this approximation,

$$\mathscr{M}_M(T) = Z_M \beta_{c,M} / Z_{Ar} \beta_{c,Ar}, \quad (1)$$

where Z_M is the collision rate coefficient. At room temperature, $F_E \approx 1$ and $F_E k_B T$ evaluates to values similar in magnitude to α such that β_c is nearly proportional to α. For large systems at high temperatures, $F_E k_B T \gg \alpha$ such that β_c is nearly proportional to α^2. We can then approximate Eq. (1) as

$$\mathscr{M}_M(T) \approx Z_M \alpha_M^n / Z_{Ar} \alpha_{Ar}^n, \quad (2)$$

with $n \approx 1$ at 300 K and $n \to 2$ at high temperature, which is easier to evaluate than Eq. (1). Here we tabulate the results of Eqs. (1) and/or (2) for a total of 37 hydrocarbons in seven atomic and diatomic baths based on values of $\alpha = \langle\Delta E_d\rangle$ obtained from ensembles of classical trajectories. Trends in $\mathscr{M}_M$ with respect to temperature, the bath gas, and the chemical structure of the unimolecular reactant are discussed. The present tabulations of $\mathscr{M}_M$ can aid in building bath gas dependence into pressure-dependent rate coefficients appearing in detailed chemical kinetic mechanisms of combustion.

The present work is organized as follows. First, a set of "universal" $C_xH_y + M$ PESs suitable for efficient classical trajectory calculations for large systems is validated against direct dynamics results. Next, Lennard-Jones collision rates Z are obtained from calculated Lennard-Jones parameters (σ and ε) for several $C_xH_y + M$ systems. A simple rule for σ and ε based only on the bath gas and the number of carbon atoms is obtained. Low-order moments of the energy transfer function are calculated using ensembles of classical trajectories. These low-order moments are used to quantify the rotational collision efficiency and to evaluate Eqs. (1) and (2) for several unimolecular reactants and for seven atomic and diatomic baths. Hydrocarbons as large as octane are considered, including linear, branched, and cyclic alkanes and linear alkenes and radicals. The dependence of $\mathscr{M}_M$ (calculated using Eqs. (1) and (2)) on temperature and the structure of the unimolecular reactant is quantified.

2. Theory

In Refs. [10] and [11], full-dimensional PESs were developed for CH_4 interacting with atomic and diatomic baths. The total PES may be written $V = V_T + V_M + V_I$, where V_T is the intramolecular potential of the hydrocarbon "target" CH_4, V_M is the intramolecular potential of the bath, and V_I is the intermolecular potential describing the target–bath interaction. In the most efficient PES previously considered by us, V_T was described via a tight binding (TB) model for hydrocarbons parameterized by Wang and Mak to reproduce molecular properties of a variety of species [15]. The diatomic bath gas intramolecular potentials, V_M, were obtained by fitting the results

Please cite this article in press as: A.W. Jasper et al., *Proc. Combust. Inst.* (2014), http://dx.doi.org/10.1016/j.proci.2014.05.105

of high-level quantum chemistry calculations to simple analytic functional forms. The results of classical trajectory calculations for collisional energy transfer relevant to unimolecular kinetics are most sensitive to V_I, which is of the same dimensionality as the full potential. A simplifying assumption involves approximating V_I as a sum of atom–atom (pairwise) Buckingham (exp/6) interactions. Buckingham parameters for CH_4 interacting with He, Ne, Ar, Kr, H_2, N_2, and O_2 were previously obtained [10,11] by fitting them to reproduce the results of high-level quantum chemistry calculations along various CH_4–bath cuts through V_I.

The resulting "separable pairwise" TB + exp/6 PESs for CH_4 + M were tested against full-dimensional, non-separable, and non-pairwise direct dynamics calculations for CH_4 + He, Ne, and H_2 by comparing low-order moments of the energy transferred in collisions [10]. The separable pairwise TB + exp/6 approach was found to predict very accurate moments for the atomic baths but was somewhat less accurate (with errors up to ~50%) for M = H_2. A parameterization for M = H_2 was obtained that reproduced the direct dynamics result.

In addition to greatly simplifying the parameterization of V_I, the separable pairwise approximation allows for the development of "universal" PESs for C_xH_y + M collisions, so long as the pairwise exp/6 parameters are transferrable from methane to the larger hydrocarbons. Here we test this transferability. Specifically, we compare the results of trajectory calculations using the TB + exp/6 PES against direct dynamics using the MP2/aug′-cc-pVDZ PES for C_2H_6 + He and C_2H_5 + He. The MP2/aug′-cc-pVDZ PES was used previously for CH_4 + He [9], where it was first validated by comparing the MP2 V_I against higher-level quantum chemistry calculations along various CH_4 + He cuts through V_I. Similar tests were repeated here for $C_2H_{5/6}$ + He, and the MP2/aug'-cc-pVDZ PES was found to have similarly good accuracy for these systems.

The "one-dimensional minimization" method [16] and the TB + exp/6 PES were used to calculate Lennard-Jones collision parameters (σ and ε) that include the effect of local anisotropy in V_I and to calculate Lennard-Jones collision rates Z. This method was previously shown to predict Z typically within 10% of collision rate coefficients based on tabulated values. The values obtained using the TB + exp/6 PES were also shown to agree well with direct MP2 and QCISD(T) calculations for several small systems.

Our strategies for calculating low-order moments of the energy transfer function from ensembles of classical trajectories have been described previously [9–11] and are used here without significant modification. Several groups have used similar classical trajectory methods in earlier studies of energy transfer (e.g., 5–8,17–20). These studies revealed many important details of the energy transfer function, including: increased energy transfer with increased initial vibrational and rotational excitation, long "tails" in ΔE corresponding to low-probability and very energetic "supercollisions [19]," and the nonseparability of ΔE and ΔJ [8]. The present ensembles typically consist of 12,800 trajectories for each unimolecular reactant, bath gas, and temperature with bootstrapped [21] 1σ statistical uncertainties of ~2%. In total, this study includes more than 3 million trajectories.

Low-order moments of the energy transfer function are typically weak functions of the initial total energy. To simplify the present study and to enable systematic comparisons between species, the initial total energies were selected close to typical threshold energies for unimolecular reactions of different classes of compounds. Specifically, the classical vibrational energies, E'_{vib}, were chosen to be independent of rotational state J' and equal to 95 kcal/mol for the alkanes and for the cycloalkanes larger than cyclobutane, 80 kcal/mol for the alkenes, 65 kcal/mol for cyclobutane, and 35 kcal/mol for the radicals. This energy includes the energy associated with the initial rotational projection quantum number K'. The initial total energy, E', is the sum of E'_{vib} and the instantaneous rotational energy for J' evaluated with $K' = 0$.

For the larger of the systems considered here, care must be taken to sample the impact parameter out to sufficiently long range. For test ensembles at 300 K and considering the normal alkanes, the impact parameter, b^*, at which the average energy transfer was less than 1 cm^{-1} was determined. For colliders other than M = He, b^* = 9–12 Å for CH_4 to C_8H_{18}, with b^* for M = He ~1 Å shorter. In the "production" trajectory ensembles, b_{max} was set to b^* + 1 Å. The values of b_{max} derived for the normal alkanes were used for the other species considered here based on the number of carbon atoms. As described previously, [9,17] the calculated moments were scaled from the trajectory-based hard-sphere collision frequency with the collision radius b_{max} to the calculated Lennard–Jones collision frequency. The present moments may then be used alongside the present calculated Lennard–Jones collision frequencies in kinetics calculations.

Vibrationally averaged rotational constants, $\langle A \rangle$ and $\langle B \rangle$, were used when selecting the initial values of J' and K' from classical thermal distributions, whereas, previously, values evaluated at the classical equilibrium geometry, A_e and B_e, were used. (A near-symmetric top is assumed for all the species considered here, where B is the average of the two most similar rotational constants, and A is the remaining rotational constant.) The vibrationally-averaged rotational

Please cite this article in press as: A.W. Jasper et al., *Proc. Combust. Inst.* (2014), http://dx.doi.org/10.1016/j.proci.2014.05.105

constants were calculated by averaging A and B evaluated at 1280 geometries sampled from a microcanonical ensemble with a total energy E' and with $J' = K' = 0$. (No attempt was made to calculate rotational-state-specific values of $\langle A \rangle$ and $\langle B \rangle$). For systems with three or fewer carbon atoms, $\langle A \rangle \approx A_e$ and $\langle B \rangle \approx B_e$. For larger systems, the vibrationally averaged rotational constants can be significantly different from A_e and B_e (as the linear alkanes coil up, e.g.). For n-octane, $\langle B \rangle / B_e = 1.5$ and $\langle A \rangle / A_e = 0.5$, where the linear equilibrium conformer was used to evaluate A_e and B_e. Because energy transfer is a sensitive function of the initial rotational quantum number, the different choices for the defining the initial distribution of J' can have a non-negligible effect on the calculated moments for the larger species.

3. Results

3.1. Validation of the universal C_xH_y + M potential

The transferability of the TB + exp/6 PES parameterization to systems larger than methane was tested for C_2H_6 + He and C_2H_5 + He. Figure 1 compares calculated values of $\langle \Delta E_d \rangle$ obtained using the analytic TB + exp/6 and direct MP2 PESs. Agreement between the results for the two PESs is typically within the error bars of the direct dynamics result. There is some indication that the TB + exp/6 PES overpredicts $\langle \Delta E_d \rangle$ for C_2H_5 + He by ~20%, particularly at low temperature. Similar studies for larger species are underway. For now, the present comparisons, along with previous tests of the TB + exp/6 PES [10,16], support its use for larger systems.

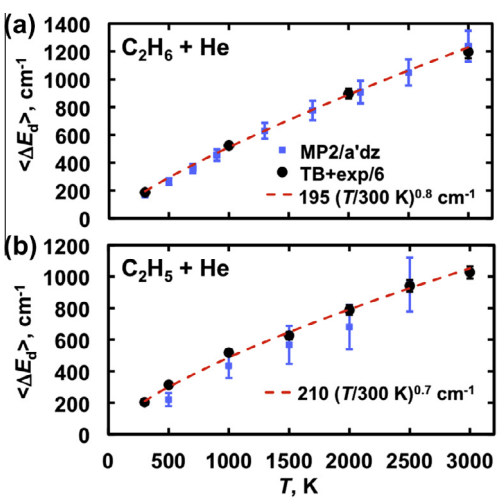

Fig. 1. The average energy transferred in deactivating collisions, $\langle \Delta E_d \rangle$, for the MP2/aug′-cc-pVDZ (blue squares) and TB + exp/6 (black circles) PESs for (a) C_2H_6 + He and (b) C_2H_5 + He. The error bars show 2σ statistical uncertainties. Simple expressions fit to the TB + exp/6 results are shown as red dashed lines. (For interpretation of the references to color in this figure legend, the reader is referred to the web version of this article.)

3.2. Collision rates

Binary Lennard-Jones collision parameters were calculated for several C_xH_{2x+2} and C_xH_{2x} species interacting with four atomic and three diatomic baths. These calculations include normal (unbranched linear), *iso*- (2-methyl), and *neo*- (2,2-dimethyl) C_xH_{2x+2} species for $x = 1$–8 and unbranched cyclic and 1-ene C_xH_{2x} species for $x = 3$–8. In total, 29 unimolecular reactants and 7 baths were considered. The predicted values of both ε and σ systematically increase with the number of carbon atoms, x, but are relatively less sensitive to branching, cyclization, and saturation. For the present set of saturated, lightly branched, and lightly unsaturated systems, we may propose $\sigma_x(\mathrm{M}) = \sigma_1(\mathrm{M}) x^{n_\sigma}$ and $\varepsilon_x(\mathrm{M}) = \varepsilon_1(\mathrm{M}) x^{n_\varepsilon(\mathrm{M})}$, where $\sigma_1(\mathrm{M})$ and $\varepsilon_1(\mathrm{M})$ are the calculated parameters for CH_4 + M, and $n_\sigma = 0.15$ and $n_\varepsilon(\mathrm{M}) = 0.25$–0.40 were fit to reproduce the results of the n-alkanes. These parameterizations reproduce the collision rates based on the explicitly calculated Lennard-Jones parameters within 5% for *all* of the collision partners considered here, including the branched, cyclic, and unsaturated species. A more detailed presentation of these results is included as supporting information.

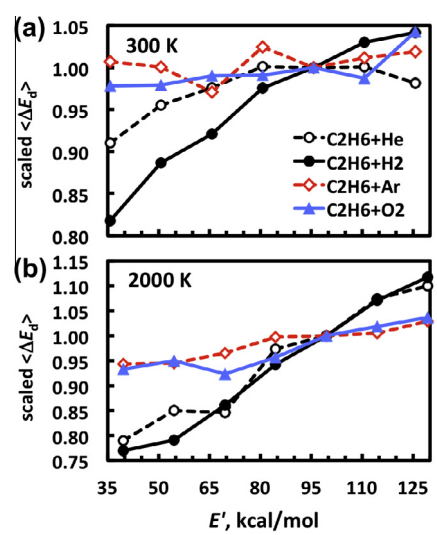

Fig. 2. The dependence of $\langle \Delta E_d \rangle$ on E' is shown for C_2H_6 in four baths at (a) 300 K and (b) 2000 K. The results for each bath gas and temperature are scaled to $\langle \Delta E_d \rangle$ for $E'_{vib} = 95$ kcal/mol.

Please cite this article in press as: A.W. Jasper et al., *Proc. Combust. Inst.* (2014), http://dx.doi.org/10.1016/j.proci.2014.05.105

3.3. Dependence on the initial energy of the unimolecular reactant

Figure 2 shows the dependence of $<\Delta E_d>$ on the initial total energy E' for C_2H_6 in He, H_2, Ar, and O_2. As expected, $<\Delta E_d>$ generally increases with E' but the dependence is minor. The results are bath gas and temperature dependent, with less dependence on E' for the heavier baths and at room temperature.

Quantifying the magnitude of the dependence of $<\Delta E_d>$ on E' is relevant to the present study as we compare collision efficiencies for species with different threshold energies. Figure 2 may be used to justify the present assumption of using "standard" threshold energies for different classes of unimolecular reactants, as differences of a few kcal/mol in the threshold energy result in negligible differences in $<\Delta E_d>$. Likewise, results for the alkanes and cycloalkanes ($E'_{vib} = 95$ kcal/mol) can be compared with those for the alkenes ($E'_{vib} = 80$ kcal/mol) with only a minor (~5%) reduction in $<\Delta E_d>$ attributed to differences in E'. When comparing results with the alkyl radicals ($E'_{vib} = 35$ kcal/mol), on the other hand, one may attribute a reduction in $<\Delta E_d>$ of ~20% for the lighter baths at high temperature to differences in E'.

3.4. Rotational collision efficiency

Next we consider the rotational collision efficiency of the seven baths for normal alkanes as large as octane. As demonstrated previously for $CH_4 + M$ [11], incomplete collisional equilibration of rotational states (i.e., weak collisions in J) can lead to a factor of ~2 reduction in the rate coefficient at 300 K relative to the results of ME models that assume complete rotational equilibration. The weak-collider-in-J effect can be estimated by comparing trajectory-based values of the average change in the rotational state in deactivating collisions, $<\Delta J_d>$, with limiting (i.e., strong-collider-in-J) values of $<\Delta J_d>$ obtained by assuming thermal or microcanonical distributions of final rotational states. As discussed previously [11], the microcanonical limit is more relevant to the 2D/φ model, whereas the thermal limit may be more relevant to the trajectory ensembles. Fortunately, both limits predict similar values of $<\Delta J_d>$, which simplifies our interpretation of the trajectory-based values of $<\Delta J_d>$. In our earlier $CH_4 + M$ study [11], water was found to be the strongest collider in J with low-order moments of ΔJ close to their microcanonical limits at low temperature (<1000 K). For $M = H_2O$ above ~1000 K and for the atomic and diatomic baths, $<\Delta J_d>$ was shown to be only 30–50% of its microcanonical limit for $CH_4 + M$.

As shown in Fig. 3, the rotational collision efficiencies of the two lightest baths, He and H_2, deviate significantly from their thermal limits

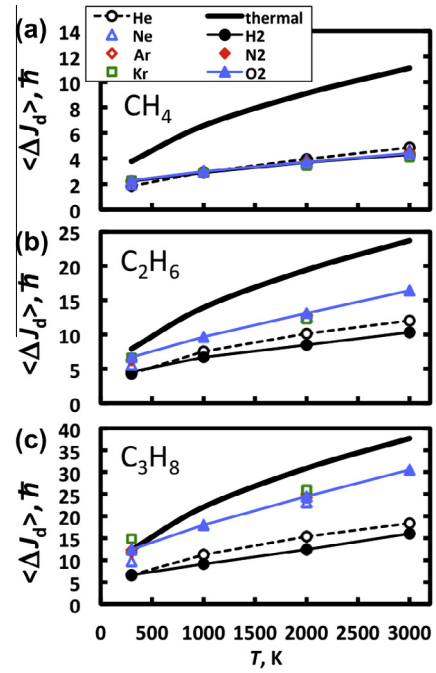

Fig. 3. The average rotational quanta transferred in rotationally deactivating collisions, $<\Delta J_d>$, for (a) methane, (b) ethane and (c) propane in seven baths. To avoid cluttering the graph, data for only three of the baths are connected with lines. Results for the larger normal alkanes are qualitatively similar to those for propane.

(which, as mentioned above, are similar to the microcanonical limiting values), even for the larger unimolecular reactants. These results suggest that an explicitly 2D model that includes this weak-collider-in-J effect may be required for quantitative predictions of these baths, although we note that the kinetic effect of weak collisions in J was previously found to be negligible above 300 K for $CH_4 + M$ [11]. The rotational collision efficiencies of the heavier baths, on the other hand, deviate significantly from their limiting values only for the smaller alkanes (methane and ethane). Results for the larger alkanes are similar to those for propane and are given as supporting information. These results suggest that the microcanonical equilibration assumption for J in the 2D/φ ME model accurately treats rotational energy transfer for the larger unimolecular reactants and the heavier baths.

3.5. Trends with respect to the bath gas

Troe's weak collider efficiencies β_c were evaluated for several normal alkanes, with $F_E k_B T = 218$–$265\ cm^{-1}$ for methane–octane at 300 K and $F_E k_B T = 1970$, 3050, 9990, 81,500, and

2,830,000 cm^{-1} for methane, ethane, butane, hexane, and octane at 2000 K, respectively. At 300 K, $F_E k_B T$ is similar in magnitude to that of α ($\alpha = 140$–$630\ cm^{-1}$ for the various baths and unimolecular reactants, with an average value of 350 cm^{-1}), resulting in near linear dependence of k_0 on α for a given unimolecular reactant. At 2000 K, $\alpha = 470$–$1250\ cm^{-1}$ with an average of 900 cm^{-1}, which is smaller than $F_E k_B T$; this results in a quadratic dependence of k_0 on α for a given unimolecular reactant. In Fig. 4, the results of Eqs. (1) and (2) are compared for a series of normal alkanes in the atomic and diatomic baths, where Eq. (2) is shown to semiquantitatively predict Eq. (1) with $n = 1$ at 300 K and $n = 2$ at 2000 K.

Results for branched, cyclic, unsaturated, and radical hydrocarbons are also shown in Fig. 4. At 300 K, $\mathscr{M}_M$ (or its approximation via Eq. (2)) depends only weakly on the chemical structure of the unimolecular reactant. The heavier atomic and diatomic baths have similar efficiencies, typically within 25% of $k_{0,Ar}$. Averaged over the 16 unimolecular reactants shown in Fig. 4, $\mathscr{M}_{Ne} = 0.76 \pm 0.03$, $\mathscr{M}_{Kr} = 0.96 \pm 0.08$, $\mathscr{M}_{N2} = 1.10 \pm 0.05$, and $\mathscr{M}_{O2} = 1.27 \pm 0.08$ at 300 K, where the uncertainty given is the standard deviation of the 16 results. For the lighter baths, $\mathscr{M}_{He} = 1.17 \pm 0.14$, with values that peak at 1.4 for the C_2 species. $M = H_2$ is the most efficient collider at 300 K, with $\mathscr{M}_{H2} = 2.49 \pm 0.44$, with maximum values near 3.3, again for the C_2 species.

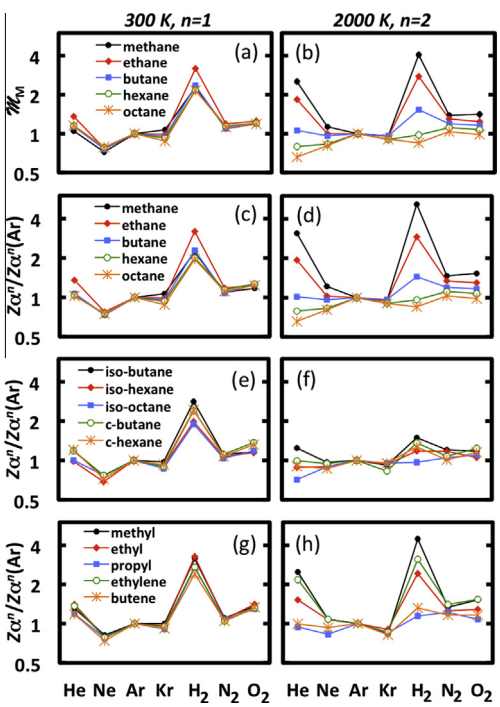

Fig. 4. Relative collision efficiencies calculated via Eq. (1) (a and b) and approximated via Eq. (2) (c–h) for normal alkanes (a–d), branched and cyclic alkanes (e and f), and alkyl radicals and alkenes (g and h), with the room temperature results ($n = 1$ in Eq. (2)) on the left and 2000 K results ($n = 2$ in Eq. (2)) on the right.

The relative collision efficiencies are functions of temperature, and the simple trends identified at 300 K do not apply at 2000 K. Aside from $\mathscr{M}_{Kr} = 0.90 \pm 0.05$, the other baths show a larger variation in their collision efficiencies with respect to the chemical structure of the unimolecular reactant at 2000 K than at 300 K. The relative collision efficiencies at 2000 K are generally functions of the number of carbon atoms for $x < 6$, with the lighter baths varying more than the heavier baths. Specifically, $\mathscr{M}_{He} = 0.66 - 3.12$, $\mathscr{M}_{Ne} = 0.81 - 1.22$, $\mathscr{M}_{H2} = 0.85 - 5.17$, $\mathscr{M}_{N2} = 1.01 - 1.47$, and $\mathscr{M}_{O2} = 0.98 - 1.54$ for the various unimolecular reactants considered here. Full tables of $\mathscr{M}_M$ are given as supporting information.

3.6. Trends with respect to the unimolecular reactant

Next trends in the collisional energy transfer with respect to the size and chemical structure of the unimolecular reactant are identified. Attention is restricted here to M = He, H_2, and O_2. For simplicity and to arrive at sensible units, we consider trends in $Zn_1\alpha$ (see Fig. 5), where n_1 is the number density of the bath gas at 1 Torr. (This choice of pressure arbitrary; different choices would uniformly scale the results in Fig. 5). This quantity includes the effects of both the collision rate and the energy transferred per collision and has units of energy transferred per time (cm^{-1}/s). Trends in $Zn_1\alpha^2$ which may be more relevant to high temperature kinetics, are qualitatively similar to those for $Zn_1\alpha$ and are not discussed.

The calculated values of $Zn_1\alpha$ generally increase with the number of carbon atoms x, with the magnitude increasing a factor of 2–5 for the different system types as x increases from 1 to 8 at the 300 K. There is less variation at 2000 K, where $Zn_1\alpha$ typically increases by less than a factor of 2 for $x = 1$–8. Results for the different bath gases are qualitatively similar to one another, but do show some quantitative differences in the magnitudes of the increases with x.

Results for the linear n-alkanes and n-alkenes are similar to one another, while the calculated values of $Zn_1\alpha$ for the branched alkanes appear shifted by ~1 carbon atom for the *iso*-alkanes and by ~2 carbons for the *neo*-alkanes, i.e., the number of carbon atoms in the *backbone* correlates better with $Zn_1\alpha$ than the total number of carbon atoms. This result can be at least partially explained by noting that the values of $\langle B \rangle$ for the *iso*- and *neo*-alkanes are similar to those of the normal alkanes with ~1 fewer carbon atom, and

Please cite this article in press as: A.W. Jasper et al., *Proc. Combust. Inst.* (2014), http://dx.doi.org/10.1016/j.proci.2014.05.105

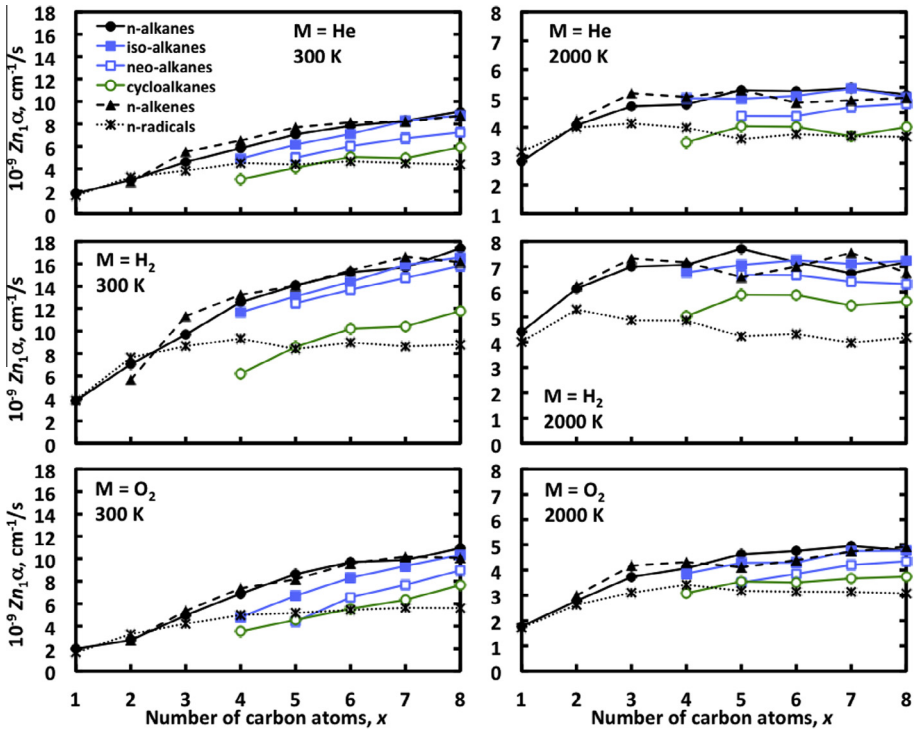

Fig. 5. Trends in $Zn_1\alpha$ as a function of the chemical structure of the unimolecular reactant in three baths and at two temperatures.

that energy transfer is a sensitive function of the distribution of J' and therefore $\langle B \rangle$.

Results for the cycloalkanes are not related to the other results in as simple a way. These results appear shifted by at least ~2 carbon atoms, but even with this shift the values of $Zn_1\alpha$ for the cycloalkanes are lower than those for the linear and branched molecular species.

Results for the n-alkyl radicals agree with those of the molecular species for small values of x (for the methyl and ethyl radicals) but are smaller than the results for the molecular systems for larger values of x. This is likely due to the lower threshold energies for the radicals, which limits the maximum amount of energy transferred in deactivating collisions. The system size at which $Zn_1\alpha$ levels off with respect to x is likely related to the tail of the energy transfer distribution getting cut off by these maxima. At 300 K, this leveling off occurs at $x = 6$ for the molecular species and at $x = 3$ for the radicals, while at 2000 K this occurs at $x = 3$ for the molecular species and $x = 2$ for the radicals. Higher temperatures and/or lower threshold energies lead to an earlier leveling off of $Zn_1\alpha$ with respect to x.

The qualitative trends identified above and shown in Fig. 5 may be useful for scaling known collision efficiencies for use in other, similar reactions.

4. Conclusions

A new set of PESs suitable for efficient trajectory simulations of large hydrocarbons colliding with any of seven atomic and diatomic baths was validated against direct dynamics calculations. The PESs were used to derive a simple and general rule for calculating Lennard-Jones parameters (and collision rates) based only on the number of carbon atoms and the bath gas. Low-order moments of the collisional energy transfer were also calculated using the new PESs for 38 unimolecular reactants in each of the 7 baths. The average angular momentum transferred in deactivating collisions was used to quantify the expected good accuracy of the simplifying assumption in the 2D/ϕ model. Relative collision efficiencies $\mathscr{M}_M$ were calculated and/or approximated for several linear, branched, and cyclic alkanes, alkenes, and alkyl radicals. Trends in $\mathscr{M}_M$ with respect to the chemical structures of the hydrocarbon reactants and temperature were identified.

Please cite this article in press as: A.W. Jasper et al., *Proc. Combust. Inst.* (2014), http://dx.doi.org/10.1016/j.proci.2014.05.105

Acknowledgments

A.W.J. was supported by the Division of Chemical Sciences, Geosciences, and Biosciences, Office of Basic Energy Sciences, U.S. Department of Energy. Sandia is a multiprogram laboratory operated by Sandia Corporation, a Lockheed Martin Company, for the National Nuclear Security Administration under contract DE-AC04-94-AL85000. C. M. O. and J.A.M. were supported as part of the Argonne-Sandia Consortium on High-Pressure Combustion Chemistry.

Appendix A. Supplementary data

Supplementary data associated with this article can be found, in the online version, at http://dx.doi.org/10.1016/j.proci.2014.05.105.

References

[1] J. Troe, *J. Chem. Phys.* 66 (1977) 4745–4757.
[2] F.J. Fletcher, B.S. Rabinovitch, K.W. Watkins, D.J. Locker, *J. Phys. Chem.* 70 (1966) 2823–2833.
[3] J.V. Michael, M.-C. Su, J.W. Sutherland, J.J. Carroll, A.F. Wagner, *J. Phys. Chem. A* 106 (2002) 5297–5313.
[4] G. Altinay, R.G. Macdonald, *J. Phys. Chem. A* 116 (2012) 1353–1367.
[5] G. Lendvay, G.C. Schatz, *J. Phys. Chem.* 96 (1992) 3752–3756.
[6] T. Lenzer, K. Luther, J. Troe, R. Gilbert, *G.; Lim, K. F, J. Chem. Phys.* 103 (1995) 626–641.
[7] I. Oref, *Isr. J. Chem.* 47 (2007) 205–214.
[8] (a) J.R. Barker, R.E. Weston, *J. Phys. Chem. A* 114 (2010) 10619–10633;
(b) J.R. Barker, R.E. Weston, *J. Phys. Chem. A* 116 (2012) 799, E.
[9] A.W. Jasper, J.A. Miller, *J. Phys. Chem. A* 113 (2009) 5612–5619.
[10] A.W. Jasper, J.A. Miller, *J. Phys. Chem. A* 115 (2011) 6438–6455.
[11] A.W. Jasper, J.A. Miller, S.J. Klippenstein, *J. Phys. Chem. A* 117 (2013) 12243–12255.
[12] J.R. Barker, D.M. Golden, *Chem. Rev.* 103 (2003) 4577–4591.
[13] M.J. Pilling, S.H. Robertson, *Annu. Rev. Phys. Chem.* 54 (2003) 245–275.
[14] J.A. Miller, S.J. Klippenstein, *J. Phys. Chem. A* 110 (2006) 10528–10544.
[15] Y. Wang, C.H. Mak, *Chem. Phys. Lett.* 235 (1995) 37–46.
[16] A.W. Jasper, J.A. Miller, *Combust. Flame* 161 (2014) 101–110.
[17] N.J. Brown, J.A. Miller, *J. Chem. Phys.* 80 (1984) 5568–5580.
[18] K.F. Lim, R.G. Gilbert, *J. Chem. Phys.* 94 (1990) 72–76.
[19] D.L. Clarke, K.C. Thompson, R.G. Gilbert 182 (1991) 357–362.
[20] O. Meroueh, W.L. Hase, *J. Phys. Chem. A* 103 (1999) 3981–3990.
[21] S. Nangia, A.W. Jasper, T.F. Miller III, D.G. Truhlar, *J. Chem. Phys.* 120 (2004) 3586–3597.